scientific reports

Check for updates

OPEN

VR-based gamma sensory stimulation: a pilot feasibility study

Carolina Reis[1✉], Hamed Azizollahi[1], Gabriel Headley[1], Sergi Navarro[1], Simon Hanslmayr[2], Andrew Clouter[3], Theodore P Zanto[4,5] & Raphael Certain[1]

Alzheimer's disease (AD) presents a critical global health challenge, with current therapies offering limited efficacy and safety in halting disease progression. Gamma sensory stimulation (GSS) has emerged as a promising non-invasive neuromodulation technique that enhances gamma neural synchrony, potentially counteracting AD pathology by promoting glymphatic clearance, reducing neuroinflammation and improving synaptic plasticity. However, existing GSS delivery methods rely on simplistic sensory stimuli that lack user engagement, potentially creating adherence barriers and limiting the full therapeutic potential of this approach. To address this, we investigated whether GSS delivered through virtual reality (VR) could safely and effectively evoke gamma-band neural activity while providing an engaging and tolerable user experience. Sixteen cognitively healthy older adults participated in a single-session, within-subject feasibility study consisting of three VR-based experiments. In each, 40 Hz auditory and/or visual stimuli were presented, and neural responses were recorded using electroencephalography (EEG). Tolerability and safety were assessed via digital questionnaires. Source-level analysis from Experiment 1 confirmed that unimodal auditory and visual stimulation at 40 Hz reliably increased gamma power in their respective sensory cortices. Sensor-level analyses from Experiments 2 and 3 showed that multimodal audiovisual stimulation enhanced both gamma power and inter-trial phase coherence—whether delivered through passive video viewing or integrated into an active cognitive task. Participants reported high comfort and engagement, with no serious adverse events. The findings of this study validate VR as a scalable tool for delivering engaging and cognitively relevant GSS, paving the way for personalized therapies that maximize adherence and therapeutic outcomes. By integrating interactive elements, VR-based GSS may uniquely target memory-related neural networks, offering a novel approach to mitigate neurotoxicity and cognitive decline in AD.

Alzheimer's disease (AD) is the leading cause of dementia worldwide, carrying a profound personal and economic burden that affects millions of families and communities[1]. Nevertheless, despite decades of research, no therapy has yet been developed that can safely provide meaningful clinical benefits while altering the progression of the disease for the vast and diverse population living with AD.

In AD, the characteristic symptoms of progressive memory loss and reduced ability to perform everyday tasks stem from multiple complex pathophysiological markers. These include the accumulation of amyloid-beta plaques and tau neurofibrillary tangles, dysregulated glial cell activity, impaired glymphatic clearance, and diminished synaptic plasticity[2–4]. Current therapeutic strategies often focus on targeting a single pathological hallmark of AD, such as amyloid-beta accumulation or neurotransmitter imbalances, without addressing the multifactorial nature of the disease. As a result, these approaches have had limited success in modifying disease progression or restoring cognitive function in a safe and effective manner. For instance, pharmacological solutions such as cholinesterase inhibitors and NMDA receptor antagonists, which have been the standard of care for decades, provide only temporary relief from cognitive symptoms and fail to address the underlying disease pathology. Conversely, recently approved intravenous drugs like Lecanemab and Donanemab, while highly effective at reducing amyloid-beta burden, offer only modest clinical benefits and are associated with significant risks, including cerebral edema and hemorrhage[5,6].

In light of these challenges, non-invasive neuromodulation techniques have emerged as promising candidates for safer and potentially more effective therapeutic options for AD[7–11]. Gamma Sensory Stimulation (GSS), in particular, has gained increased attention due to its potential disease-modifying effects, high safety profile,

[1]Clarity Health Technologies, Inc, Wilmington, DE, USA. [2]Centre for Neurotechnology, School of Psychology and Neuroscience, University of Glasgow, Glasgow, UK. [3]Department of Psychology, Nottingham Trent University, Nottingham, UK. [4]Department of Neurology, University of California-San Francisco, San Francisco, CA, USA. [5]Neuroscape, University of California San Francisco, San Francisco, CA, USA. ✉email: carolina@clarity-technologies.com

and suitability for at-home use[12–15]. GSS employs flickering lights and/or pulsing sounds at 40 Hz to enhance neural synchrony at gamma frequencies. Gamma oscillatory activity plays a critical role in cognition, with inter-areal gamma synchronization consistently linked to functions such as attention and memory across species[16–19]. Notably, this synchrony is disrupted in Alzheimer's disease, suggesting a potential mechanism underlying cognitive decline[20,21]. When applied over prolonged periods, GSS appears capable of modulating key disease mechanisms in a safe and impactful manner. Compellingly, data from a Phase II clinical trial demonstrated encouraging results, with daily GSS for one hour over six months reducing brain atrophy by 69% and preserving cognitive and functional abilities by approximately 76% in the active treatment group, compared to the placebo group, in a cohort of mild-to-moderate AD patients[15]. Importantly, this same study highlighted GSS's excellent safety profile, reporting no severe adverse events and only mild to moderate adverse events that resolved quickly[15].

These promising clinical outcomes are likely driven by the multifaceted impact GSS has on pathological processes in AD, as supported by a rapidly growing body of research. At the cellular and systemic levels, preclinical and clinical studies indicate that GSS enhances glymphatic clearance and recruits glial cells—such as microglia and astrocytes - facilitating the removal of neurotoxic proteins such as amyloid-beta, restoring homeostasis, reducing neuroinflammation, and slowing down neurodegeneration[22–26]. At the network level, GSS is thought to recover disrupted communication pathways by promoting gamma synchronization within sensory regions and across interconnected brain areas[27]. This synchronization supports cognitive functions and mechanisms like synaptic plasticity, which are critical for learning and memory formation[28,29].

However, despite its promise, current delivery methods for GSS, aimed at being prescribed as an at-home non-invasive neuromodulation approach, face significant limitations that may hinder its full therapeutic potential. Much like in drug discovery—where dosage, timing, and molecular targets must be carefully calibrated—neuromodulation requires optimized parameters, including intensity, frequency, and target brain regions to recover behavior[30]. At present, most GSS solutions rely on passive, repetitive stimuli delivered through basic technologies like Light-Emitting Diodes (LEDs) alone or in combination with audio speakers. While effective at inducing gamma neural activity, these static designs might lack the cognitive engagement necessary to maximize therapeutic efficacy and sustain adherence, especially for long-term, at-home use, as suggested by the dropout rate of 28% reported in a six-month phase II study[31].

The magnitude and spread of neural entrainment significantly depend on the relevance of, and attention given to, the external stimuli. Recent advances in frequency tagging paradigms have demonstrated that entrainment is both content- and region-specific, with selective enhancement when the tagged stream is attended. For example, during an object-based attention paradigm, frequency-tagged faces and houses elicited dissociable responses in category-selective regions such as the fusiform face area and parahippocampal place area. Crucially, when attention was directed to one of the object categories, the neural response was amplified in its corresponding cortical region[19]. Similarly, when distinct features of a composite face are flickered at different frequencies, selective attention enhances the frequency-tagged response of the task-relevant feature in corresponding face-selective areas[32]. This attentional modulatory effect has also been observed in paradigms employing quasi-rhythmic stimuli, where spatial attention showed to enhance neural tracking of contrast fluctuations across visual cortical regions[33]. Collectively, these findings suggest that attention not only sharpens local entrainment but also facilitates its integration into distributed, task-relevant networks—an effect that appears critical for driving stimulation deeper into cognitive circuits. Supporting this, Khachatryan and colleagues (2022) showed that gamma activity in the hippocampus, a region essential for memory and highly affected in AD, was only evoked when visual GSS was paired with cognitively engaging tasks, such as visual attention or mental counting. Passive stimulation alone failed to elicit such responses, emphasizing that attentional engagement may be a prerequisite for effective gamma propagation into memory-related structures[34]. Although other studies suggest that current plain and context-irrelevant GSS methods can evoke gamma activity in broader memory-related networks, such as the medial temporal lobe-prefrontal cortex (MTL-PFC) network and the default mode network (DMN)[27,35] we hypothesize that these effects may be limited in scope. Simple, passive 40 Hz flickers and tones, when delivered continuously for an hour, may not robustly or consistently engage critical deep brain regions like the hippocampus, reducing the overall impact of GSS on cognitive decline. Such a scenario would potentially help explain the mixed cognitive outcomes observed in prior studies. Notably, while the previously mentioned Phase II trial showed significant improvements on the Mini-Mental State Examination (MMSE), it failed to achieve meaningful gains on its primary endpoint - Alzheimer's Disease Assessment Scale-Cognitive Subscale (ADAS-Cog), a cognitive assessment that evaluates higher-order cognitive functions such as memory and executive processing and which is largely considered the gold standard for evaluating cognitive decline in AD[15]. This discrepancy likely reflects the inability of passive GSS to effectively engage the networks underpinning these cognitive domains. Additionally, the monotony of current GSS protocols risks fluctuations in arousal states, potentially compromising the consistency of neural entrainment[36] and, consequently, therapeutic outcomes. This challenge is particularly significant in at-home settings, where maintaining sustained engagement is crucial for ensuring a positive patient experience and adherence to treatment.

To address these limitations, we propose integrating 40 Hz sensory stimulation into immersive and interactive VR environments as an innovative strategy to enhance the clinical efficacy of GSS and support sustained adherence in home-based settings. VR offers a uniquely immersive and controllable multisensory environment that may enhance the efficacy of sensory stimulation by increasing perceptual salience, attentional engagement, and ecological validity. VR is increasingly used in neuroscience research and clinical interventions, including the treatment of chronic pain, stroke rehabilitation and phobias, due to its capacity to simulate realistic, task-relevant environments and engage distributed cognitive and sensory systems[37,38]. In line with this vision, the current pilot study evaluates the feasibility, safety, and tolerability of using VR technology to deliver GSS in cognitively healthy older adults. Using EEG recordings, we assessed changes in gamma rhythms during three

Adverse events ($n = 16$)	Null *n*. participants (% participants)	Mild *n*. participants (% participants)	Moderate *n*. participants (% participants)
General discomfort	7 (43.7%)	8 (50%)	1 (6.3%)
Headache	12 (75%)	4 (25%)	-
Tinnitus	16 (100%)	-	-
Eye pain	14 (87.4%)	1 (6.3%)	1 (6.3%)
Disorientation	15 (93.7%)	1 (6.3%)	-
Fatigue	5 (31.2%)	7 (43.8%)	4 (25%)
Nausea	16 (100%)	-	-
Blurred vision	10 (62.5%)	6 (37.5%)	-

Table 1. Results from the safety questionnaire completed by 16 cognitively healthy older participants.

Demographics	
Age (mean, SD)	77.3 ± 11.0 years
Female sex (n, %)	13 (81.3%)
Years of education (mean, SD)	17.8 ± 2.1 years
Reported race: white (n, %)	15 (93.8%)
MoCA (mean, range)	28.3 (26–30)
GDS (mean, range)	0.9 (0–3)

Table 2. Demographics and baseline clinical characteristics of cognitively healthy older participants ($n = 16$).

VR-based stimulation tasks and collected safety and tolerability data through a digital questionnaire. This proof-of-concept study aims to lay the groundwork for developing user-friendly and contextually relevant VR-based GSS interventions, potentially transforming AD care by providing a widely accessible and potentially disease-modifying treatment to the growing and diverse population affected by the disease.

Results

VR-based gamma sensory stimulation is safe and well-tolerated

Safety and tolerability assessments from the digital questionnaires completed by all 16 participants at the end of the experimental session revealed that our VR-based gamma sensory stimulation protocol was well-received, with no severe adverse events reported (see Table 1 for a summary of reported symptoms, their severity ratings, and frequency across participants). Notably, no participants experienced motion sickness, underscoring the feasibility of integrating sensory stimulation protocols with VR technology. Participant demographics and eligibility criteria are detailed in the Methods section and summarized in Table 2.

Tolerability results further highlighted the acceptability of the stimulation method. Most participants found the headset comfortable, with 68.8% rating it 5 or higher on a 7-point scale (1 = "not at all comfortable" and 7 = "extremely comfortable"), and the VR experience was rated as enjoyable, with no participant giving a score below 4 (4 = "neutral enjoyment"). Additionally, 93.8% of participants found the VR environment manageable and non-overwhelming, rating it 2 or lower on a 7-point scale (1 = "not at all overwhelming" and 7 = "extremely overwhelming"), with only one participant score of 4.

These findings demonstrate that our VR-based GSS approach provided a safe and balanced immersive experience suggesting its viability for extended use. Although this study primarily assessed feasibility with added equipment (EEG cap and VR headset) and multiple experimental tasks instead of a complete therapeutic protocol, these preliminary results provide a solid foundation for the development of a scalable, safe, and effective therapeutic application.

VR-based gamma sensory stimulation leads to significant modulation of gamma activity

Experiment 1 assessed the ability of VR technology to drive neural activity at gamma rhythms by separately presenting distinct visual and auditory stimuli. See Fig. 1 and Methods for full details on the experimental paradigm. As results, both sensor-level (Fig. 2A, B, and C) and source-level (Fig. 2D) analyses confirmed that our VR-based GSS protocol was capable of effectively enhancing gamma oscillatory activity. This enhancement was evidenced by the clear spectral peak at 40 Hz (dashed vertical line) in the average power spectral density curves during active stimulation, and its absence during baseline periods (Fig. 2A and C).

Further analysis revealed that all stimuli modulated at 40 Hz - whether simple or complex, auditory or visual - elicited a significant increase in gamma power from baseline. At the group level, fold-changes (FC) from baseline in gamma power were observed at sensor locations relevant to the modality: Oz, PO3, PO4, and POz for visual stimuli, and Cz, C2, C1, and FCz for auditory stimuli. Specifically, auditory stimuli showed significant gamma power increases for both 40 Hz click trains and pure tones amplitude-modulated at 40 Hz, with no significant difference in the magnitude of their effects (FCclicks = 0.19, $p < 0.001$; FCpure tones = 0.17; $p < 0.001$; difference
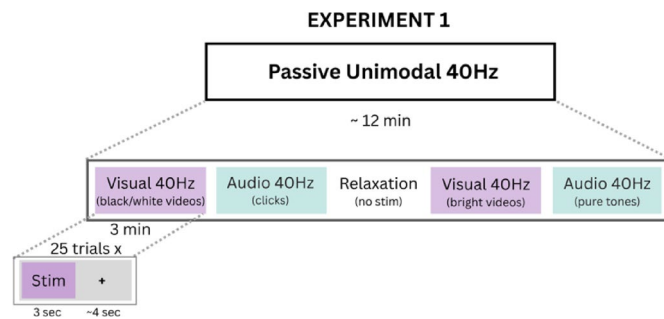
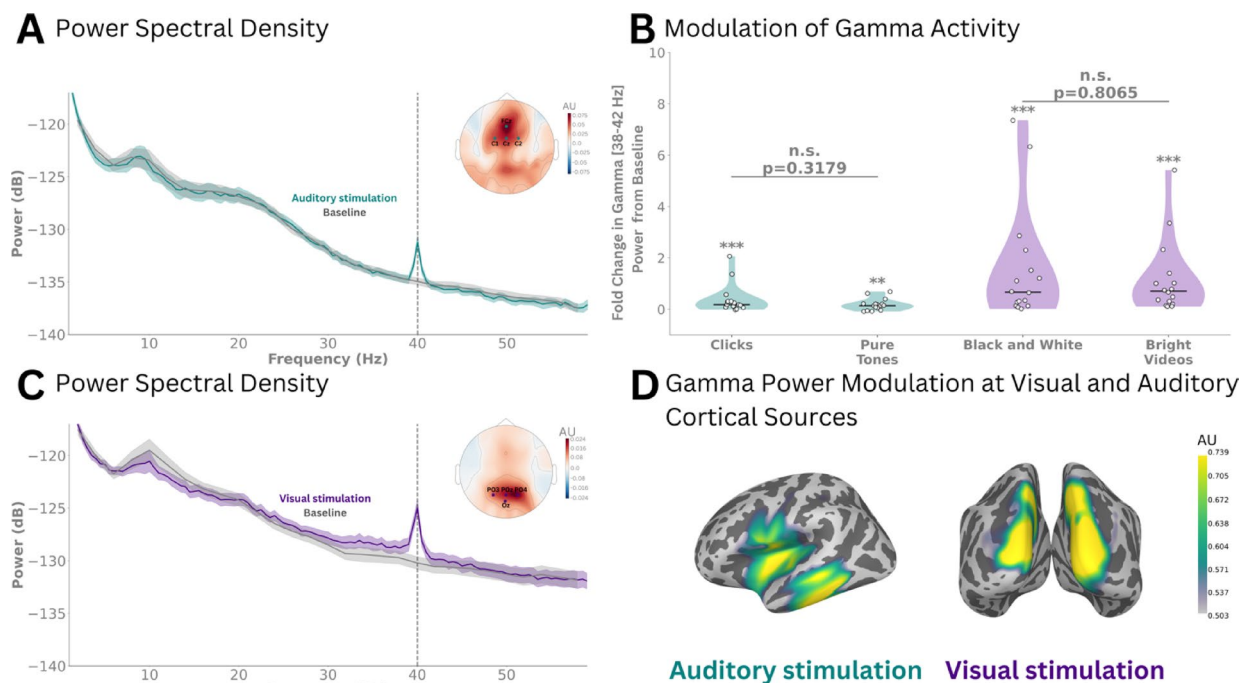**Fig. 1**. Experimental paradigm 1: passive unimodal 40 Hz stimulation.

Fig. 2. Gamma power modulation during auditory and visual VR-based 40 Hz stimulation. (**A**) Power spectral density analysis comparing auditory stimulus (green) and baseline periods (grey) across frontocentral channels (Cz, C2, C1, and FCz). The plot shows grand average power spectra as full lines and shaded areas represent the standard error of the mean. The topo map depicts the spatial distribution of changes in gamma band (38–42 Hz) power at the sensor level using baseline corrected log power ratio. The color scale represents the relative change in power from baseline, where darker blue indicates lower power and red indicates higher power. (**B**) Comparison of gamma band (38–42 Hz) power changes across different sensory stimulation conditions. Violin plots represent power changes for auditory conditions (green: Clicks, Pure Tones) and visual conditions (purple: Black and White, Bright Videos), where the horizontal line represents the median, overlaid circles are individual subjects, and individual significance is indicated by asterisks (*$p < 0.05$, **$p < 0.01$, ***$p < 0.001$). (**C**) Same as (**A**) but for visual stimulation and across parietooccipital channels (POz, PO3, PO4, Oz). (**D**) Cortical source localization of gamma power during auditory (green) and visual (purple) stimulation, highlighting modality-specific cortical gamma modulation. The figure shows DICS beamformer source reconstruction of gamma band (40 Hz) activity, comparing stimulation to baseline periods. Color intensity represents the log-transformed power ratio (dB) between stimulation and baseline periods.

between FCclicks and FCpure tones = 0.02, $p = 0.318$). Similarly, visual stimuli demonstrated significant gamma power increases for both black-and-white videos and random bright videos (FCblack-and-white videos = 0.52, $p < 0.001$; FC random bright videos = 0.54, $p < 0.001$), with no significant difference in gamma power increases between the two types of visual stimuli (difference between FCblack-and-white and FCrandom bright videos = -0.02, $p = 0.8065$).

Source-level analysis further localized the increase in gamma activity to the primary auditory and visual cortical areas for the auditory and visual stimuli, respectively (Fig. 2D). This finding confirms the specificity of the neural response observed in previous analyses and rules out contributions from muscular activity (e.g., eye
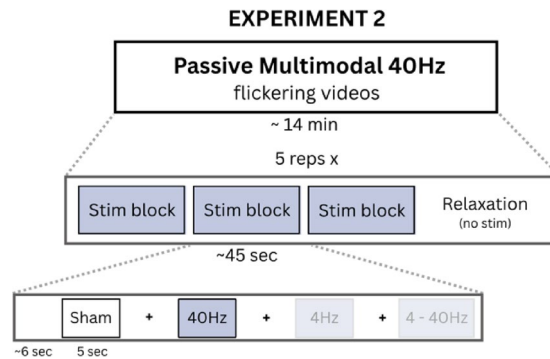
Fig. 3. Experimental paradigm 2: passive multimodal 40 Hz stimulation.
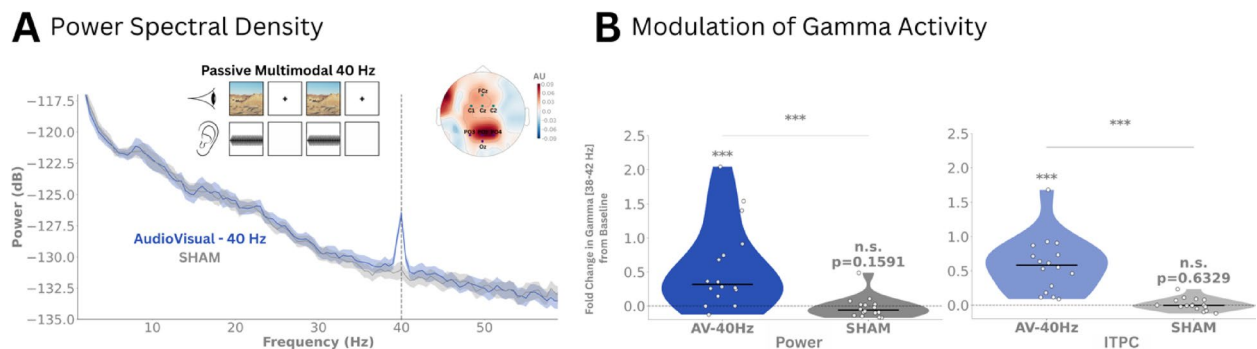

Fig. 4. Modulation of gamma neural activity in response to audiovisual VR content modulated at 40 Hz. (**A**) Group-level PSD comparison between 40 Hz audiovisual stimulation and sham conditions. The plot shows grand average power spectra (± SEM, shaded areas) across frontocentral and parietooccipital channels (FCz, C1, C2, Cz, Oz, PO3, PO4, POz) for the 40 Hz stimulation condition (labelled as AudioVisual-40 Hz stimulation and shown in blue) and sham condition (labelled as SHAM and shown grey). The topo map depicts the spatial distribution of power change in gamma band (38–42 Hz) at the sensor level using baseline corrected log power ratio. The color scale represents the relative change in power from baseline, where darker blue indicates lower power and red indicates higher power. A simplified illustration of the experimental task is shown in the same panel, depicting the VR content—video and corresponding sound waveform—either modulated at 40 Hz or left unmodulated, which was passively observed by participants during Experiment 2 (passive multimodal 40 Hz stimulation), as described in the Methods section. (**B**) Fold change in gamma-band power (left) and inter-trial phase coherence (ITPC; right) between stimulation and baseline periods for the AV-40 Hz (blue) and sham (grey) conditions is shown across the same channels. Violin plots display individual data points (white circles), group medians (horizontal lines), and distribution widths. Significant differences are indicated by asterisks (*$p < 0.05$, **$p < 0.01$, ***$p < 0.001$).

squinting due to the flicker or neck tension from the headset weight), which would typically be registered over the pre-central gyrus.

Together, these findings underscore the ability of VR-based stimulation to reliably modulate gamma activity across diverse stimulus types, whether simple or complex, in both auditory and visual modalities.

In Experiment 2, we evaluated the feasibility of delivering audiovisual stimulation through VR technology and sought to validate that the observed gamma activity was driven by external 40 Hz modulation rather than endogenous sensory processing[39–42]. This was achieved by comparing neural responses under two conditions: brightness and sound volume modulated at 40 Hz (active condition) versus no modulation (sham condition), and by measuring neural responses as fold-change from baseline not only in gamma power but also in Inter-Trial Phase Coherence (ITPC) at gamma frequencies. See Fig. 3 and Methods for full details on the experimental paradigm.

Similar to the results obtained under unimodal conditions, multimodal 40 Hz stimulation significantly enhanced gamma activity, as shown by a prominent spectral peak at 40 Hz in the PSD present only for the active condition (Fig. 4A). Moreover, both gamma power and ITPC increased significantly from baseline in the active condition (FC power AV-40 = 0.32, $p < 0.001$; FC ITPC AV-40 = 0.58, $p < 0.001$), while no significant changes were observed in the sham condition (FC power Sham = -0.06, $p = 0.159$; FC ITPC Sham = 0.00, $p = 0.633$) (Fig. 4B).

Figure 5, depicts a single-participant analysis highlighting the spatial localization of the 40 Hz stimulation at the sensor level and its temporal stability. Similarly to Fig. 4A, Fig. 5A shows a 40 Hz spectral peak during stimulation but not during baseline. Additionally, the polar plots in Fig. 5B illustrate the distribution of phase
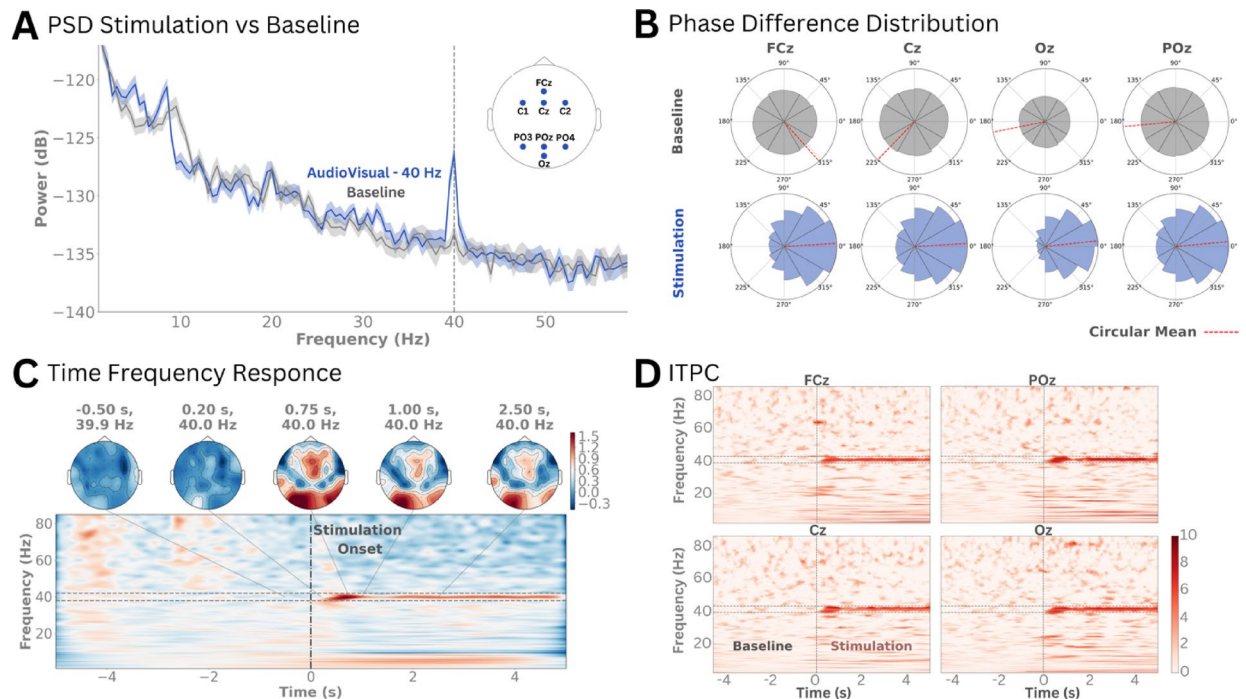
Fig. 5. Individual subject results for 40 Hz audiovisual stimulation. (**A**) PSD comparison between 40 Hz audiovisual stimulation (blue) and baseline (grey). Shaded areas represent the standard error of the mean and full lines the mean power spectral density across trials. (**B**) Phase difference polar plots for selected electrodes (FCz, Cz, Oz, POz) comparing baseline and stimulation periods. The polar histograms show the distribution of instantaneous phase differences across multiple trials in 12 bins from -π to π. Top row displays baseline period phase distributions (grey), while bottom row shows stimulation period phase distributions (blue). Red dashed lines indicate circular means of phase angles. (**C**) Joint visualization of time-frequency power changes and corresponding topographical distributions during 40 Hz stimulation. Top row shows topographical maps of power distribution at five time points relative to stimulation onset. The topographic map uses a color scale ranging from -0.3 (blue) to 1.5 (red), representing log-ratio power changes relative to baseline, with white indicating no change (0). The main panel shows the time-frequency representation of power changes across the epoch (-5 to 5s), with horizontal dashed lines indicating the gamma band of interest (38–42 Hz) and vertical dash-dotted line marking stimulation onset (0s). (**D**) Inter-trial phase coherence during audio-visual stimulation for four selected EEG channels (FCz, Cz, Oz, POz). Time-frequency representations show ITPC computed using Stockwell transform (1–85 Hz). The data is baseline corrected and displayed in z-scores using a red colormap (0 to 10). Grey dashed lines indicate the frequency band of interest (38–42 Hz). Higher ITPC values (darker red) represent stronger phase consistency across trials at specific time-frequency points.

differences in gamma rhythmic activity (38–42 Hz) across trials during pre- and post-stimulation periods. The results reveal a consistent phase alignment across trials, particularly in frontocentral and parietooccipital electrodes, as indicated by the clustering of phase differences around 0 degrees and the circular mean phase difference close to 0 degrees. Time-frequency (Fig. 5C) and ITPC plots (Fig. 5D) confirm sustained gamma power increases and phase-locking during the stimulation window, in line with our group-level results.

Altogether, these findings demonstrate that VR-based 40 Hz multisensory stimulation effectively evokes robust oscillatory activity at gamma frequencies, confirming its efficacy in multimodal conditions.

In Experiment 3, we assessed whether loosely controlled multimedia content, modulated at 40 Hz and integrated into a video-sound associative memory task, could effectively drive gamma neural activity. The experimental design is described in the Methods section and illustrated in Fig. 6. As shown in Fig. 7, both gamma power and ITPC significantly increased during the active 40 Hz modulation condition compared to baseline (FC power AV-40 = 0.17, $p < 0.01$; FC ITPC AV-40 = 0.29, $p < 0.001$), with no significant changes observed in the sham condition for either metric (FC power Sham = -0.03, $p = 0.579$; FC ITPC Sham = 0.0, $p = 0.873$). Moreover, the increases in gamma power and ITPC during the active condition were significantly greater than those in the sham condition ($p < 0.01$). A secondary aim of this task consisted of testing whether content flickered at 40 Hz versus non-flickered content (sham condition) during the encoding phase of the associative memory task led to higher levels of recall accuracy. We found no significant differences in the percentage of correct recall trials between the two conditions (mean ± SD accuracy for the active and sham conditions: 64% ± 10% and 66% ± 11%, respectively; $p = 0.372$). Importantly, while these findings do not demonstrate an immediate effect on recall accuracy, they do not preclude the possibility that prolonged application of these protocols could yield cognitive and neuroprotective benefits for AD patients, as further explored in the discussion section.
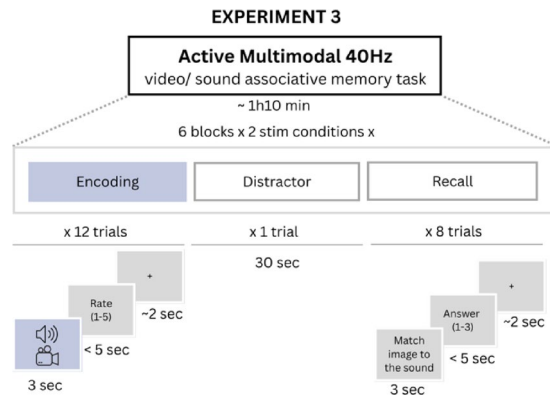
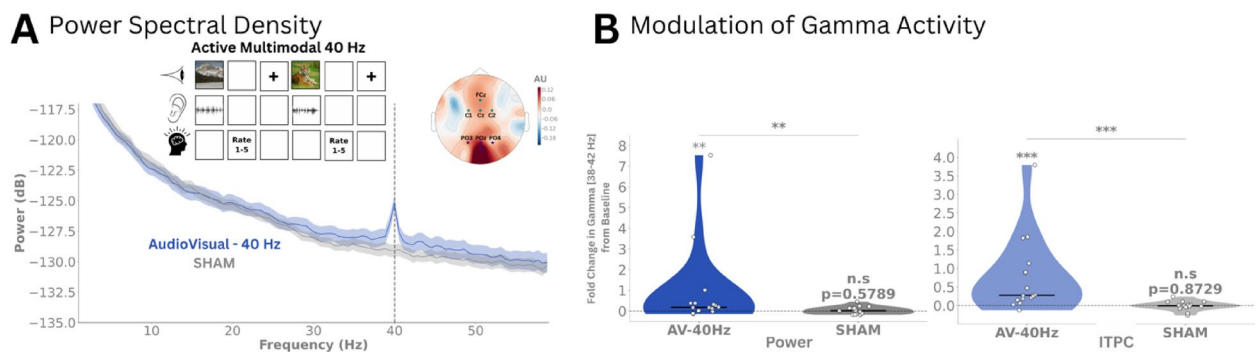**Fig. 6.** Experimental paradigm 3: active multimodal 40 Hz stimulation.

Fig. 7. Modulation of gamma neural activity in response to task-based VR Gamma Sensory Stimulation. (**A**) Group-level PSD comparison between 40 Hz audiovisual stimulation and sham conditions. The plot displays grand average power spectra (± SEM, shaded regions) across selected channels (FCz, C1, C2, Cz, Oz, PO3, PO4, POz). Power spectra are illustrated for the 40 Hz stimulation condition (labeled as AudioVisual-40 Hz stimulation and represented in blue) and the sham condition (labeled as SHAM and depicted in grey). The topo map depicts the spatial distribution of power modulation in gamma band (38–42 Hz) at the sensor level using baseline corrected log power ratio. The color scale represents the relative change in power from baseline, where darker blue indicates lower power and red indicates higher power. A simplified illustration of the task is shown in the same panel, depicting the audiovisual content flickered during the encoding phase of an associative memory task (Experiment 3: active multimodal 40 Hz stimulation; see Methods for more details). (**B**) Fold change in gamma-band (38–42 Hz) power (left) and inter-trial phase coherence (ITPC; right) from baseline across the same channels. Violin plots display individual subject data (circles) and group medians (horizontal lines) for AV-40 Hz (blue) and sham (grey) conditions. Asterisks denote statistically significant differences (*$p < 0.05$, **$p < 0.01$, ***$p < 0.001$); "n.s." indicates non-significant comparisons.

These findings demonstrate that a reliable increase in gamma activity can be achieved even with multimedia content featuring varying brightness levels, auditory complexity, and naturalistic characteristics. This marks an important step toward developing flexible VR-based therapies that maintain effective modulation of gamma brain rhythms while fostering greater patient engagement and adherence through more immersive and cognitively-relevant GSS protocols.

Discussion

This feasibility study demonstrates that VR technology can effectively deliver gamma sensory stimulation. In a cohort of 16 cognitively healthy older adults, we showed that 40 Hz-modulated audiovisual content, delivered under both passive and cognitively demanding conditions, successfully and safely evoked gamma oscillatory activity. These findings establish a strong proof of concept for leveraging VR technology into engaging and cognitively relevant GSS interventions aimed at enhancing both the therapeutic efficacy and adherence of current GSS approaches.

From a safety perspective, the absence of severe adverse events aligns with prior findings from a six-month trial investigating self-administered daily GSS in mild to moderate AD[15]. In the current study, the most frequently reported side effects, including mild headaches, general discomfort, and fatigue, were transient and are most likely attributable to the experimental setup, which involved multiple tasks and the use of an EEG cap, headphones, and a VR headset. This suggests that these effects are unlikely to stem from the neuromodulation

approach itself and emphasizes the need for longitudinal trials with less burdensome setups to further assess tolerance and patient adherence to VR-based GSS. Tinnitus, a phantom auditory perception characterized by a persistent ringing or buzzing in the ears, has been reported as a side effect in previous studies of GSS. It occurred in 15% of participants in the active group of a Phase II trial[15] and was linked to worsened pre-existing tinnitus in one feasibility study participant after a single session[43]. However, in our study, no tinnitus was observed, even in a participant with a history of the condition. Lastly, the safety results from this study suggest that strategies like implementing a gradual off-boarding process to help participants readjust to their surroundings and using VR-specific lenses to reduce visual strain could effectively mitigate transient side effects such as disorientation and blurred vision in future applications.

Efficacy-wise, this study demonstrated that VR-based GSS can drive gamma activity, with effects observed across different sensory modalities, stimulus complexities, and tasks with varying cognitive demands. Both visual and auditory stimulation independently induced significant gamma oscillatory activity, as evidenced by significant fold changes in power from baseline within corresponding sensory cortical regions (Fig. 2). Importantly, the study also highlighted the design flexibility of VR-based GSS since directly comparing simple stimuli, such as black-and-white flickers and 40 Hz clicks, with complex stimuli, including bright videos and amplitude-modulated pure tones, revealed no significant differences in gamma power increase (Fig. 2B). This suggests that engaging, contextually-rich content can be paired with gamma stimulation without significantly diminishing its efficacy, offering exciting opportunities for personalized, user-friendly interventions that promote adherence and therapeutic engagement.

When delivering auditory and visual 40 Hz stimuli simultaneously, we evaluated gamma activity modulation under both controlled and naturalistic conditions, employing passive as well as cognitively engaging GSS protocols. Controlled scenarios employed repetitive multimedia content presented with and without 40 Hz modulation, while naturalistic conditions involved varied 40 Hz modulated and unmodulated audiovisual pairs in an associative memory task. Across both paradigms, our VR-based GSS approach reliably modulated gamma neural activity, evidenced by significant increases in both power and temporal alignment during the active condition compared to the sham (Figs. 4, 5 and 7). While our protocol was not powered to systematically compare the effects of audiovisual material flickered at 40 Hz with varying cognitive loads on gamma modulation, it highlights an important avenue for future research. In addition, we observed considerable inter-subject variability in gamma-band responses, reflected in both power and phase coherence metrics. This likely stems from differences in neural responsiveness, anatomical variation, and headset or EEG cap fit. While group-level effects were robust, future studies may benefit from stratifying participants or employing adaptive stimulation protocols that account for individual neural responses. Better understanding this variability will be key to optimizing GSS interventions for clinical use.

Behavioral effects of non-invasive neuromodulation interventions are generally expected to emerge from prolonged exposure rather than a single session[12,44,45]. Nonetheless, given the critical role of gamma synchrony in binding information across brain regions, and its association with the precise temporal coordination of neuronal assemblies involved in encoding[46] we explored whether modulating the volume and brightness of video-sound pairs at 40 Hz could facilitate memory formation. Despite finding no significant differences in recall accuracy between modulated and unmodulated trials of our associative memory task, further analyses are warranted. Specifically, and consistent with previous research[29,47] assessing the strength of evoked gamma synchrony between auditory and visual cortical sources and its relationship to memory performance will be crucial for testing the hypothesis that stronger gamma synchrony induced by GSS enhances the integration of visual and auditory streams, ultimately facilitating memory formation.

Overall, our feasibility findings validate VR technology as a flexible and versatile neuromodulation tool capable of delivering auditory and visual sensory stimulation independently or in combination, embedded in diverse multimedia content and during passive or cognitively active states. The importance of such flexibility lies in the ability to strategically embed stimuli in contextually relevant content, which previous studies suggest can shape the propagation and magnitude of neural entrainment to sensory stimulation. For instance, in a study by Khachatryan et al., (2022), EEG recordings from 15 healthy young participants during 40 Hz visual stimulation showed that the topography of entrained electrodes during 40 Hz visual stimulation varied significantly depending on the cognitive task paired with the stimulation—mental counting predominantly activated parietocentral regions, while visual attention tasks engaged centrofrontal areas[34]. Similarly, sensory stimulation delivered at 5 Hz to six drug-resistant epileptic patients entrained deep brain regions, such as the hippocampus and the amygdala, only when the emotional valence of the flickered stimuli was non-neutral, and not when it was neutral[48]. Crucially, the same study found that stimuli valence influenced not only the topography of gamma modulation but also behavioral outcomes. Specifically, in a complementary experiment involving 27 healthy participants, the study reported that negative valence stimulation, but not stimulation with a neutral valence, selectively enhanced recognition memory for target items encountered during the stimulation period compared to distractor items[48]. These findings highlight the potential of incorporating contextually rich content into sensory stimulation to target specific brain networks linked to particular symptoms of AD. By leveraging these insights, VR-based GSS stands as a promising platform for advancing precision medicine in AD care, offering the potential to deliver the neuroprotective and synaptic plasticity-enhancing benefits of GSS to specific brain regions, effectively addressing distinct, patient-specific cognitive and functional deficits, and optimizing therapeutic outcomes.

Whether VR-based GSS would be well-accepted for daily at-home use by an AD population remains to be tested in future longitudinal studies; however, results from this pilot study are encouraging. While older adults are often thought to be less receptive to advanced technologies like VR, our findings challenge this notion, with ~94% of participants describing the VR experience as non-overwhelming. Additionally, despite the repetitive nature of the three experimental tasks which averaged to a total approximate duration of 1h30 and which did not

represent a fully optimized therapeutic protocol, more than half of the participants (~63%) rated the experience as enjoyable. These results align with studies showing that VR-based interventions can enhance cognitive engagement and emotional well-being in older populations, even among individuals with subjective or objective cognitive impairments[49,50]. Furthermore and in support of the VR task-based GSS approach proposed above, immersive VR environments have also been shown to offer meaningful cognitive training and rehabilitation experiences, with users reporting positive emotional responses and minimal adverse effects[51,52].

Lastly, the complete absence of motion sickness symptoms in our cohort is of particular importance, given its prevalence in VR applications[53]. This favorable outcome likely stems from deliberate design and hardware choices, including presenting 40 Hz-modulated content in 2D to create a stable, theater-like experience, and utilizing low-persistence fast switching LCD screens that minimize motion blur and enhance visual clarity.

While this study provides a critical proof of concept for VR-based gamma sensory stimulation (GSS), a few limitations should be acknowledged. As gamma sensory stimulation gains recognition for its therapeutic potential, there is increasing interest in translating this method into accessible, user-friendly solutions. However, rigorous testing of the technology used is essential to ensure therapeutic safety and efficacy. VR headsets, originally designed for interactive gaming and entertainment, are not inherently optimized for precision neural stimulation. While our experimental set up did not allow for simultaneous acquisition of stimuli and neural data, we systematically evaluated the performance of off-the-shelf VR devices using Arduino-based sound and light sensors before and after each session. These tests demonstrated that the VR-based GSS protocol used in this study could reliably deliver 40 Hz stimulation as evidenced by the average PSD peak of 39.95 ± 0.67 Hz and 40.43 ± 0.52 Hz for visual and auditory stimuli, respectively. However, phase synchrony analysis comparing a simulated 40 Hz sinusoidal waveform to visual stimulation trials recorded with a photodiode indicated relatively low stability in the visual stimulation - PLV (Phase Locking Value) = 0.65 ± 0.16. While this did not hinder our stimulation approach from driving gamma neural activity in response to visual 40 Hz stimulation (Fig. 2A,B), these findings highlight opportunities to further refine VR technology for neuromodulation applications. In addition, following the positive results of this pilot study, the safety, efficacy, and tolerability of VR-based GSS must be investigated longitudinally in a double-blind and sham controlled study and in a diverse cohort of people with AD.

Altogether, this single-day study demonstrates that VR technology can effectively deliver gamma sensory stimulation. Using 40 Hz-modulated audiovisual content, both passive and cognitively engaging conditions successfully and safely modulated gamma-frequency neural activity. The flexibility of this approach supports the development of engaging and potentially more effective GSS protocols, paving the way for scalable and personalized therapies to address the unmet needs of Alzheimer's disease and other neurodegenerative disorders.

Methods
Participants
This pilot feasibility study employed a within-patient design, where all participants were exposed to both active and sham conditions during a single study session. The study was conducted at The Sequoias Portola Valley, a senior living facility in California, and adhered to ethical guidelines, including the principles of the Declaration of Helsinki and the International Conference on Harmonization Good Clinical Practice guidelines. Ethical approval was obtained from the appropriate institutional review board and local ethics committee. All participants, or their legal representatives, provided written informed consent prior to participation, and withdrawal from the study was permitted at any time without prejudice.

A total of 16 cognitively normal older adults met the eligibility criteria and completed the study, with no participant dropouts (demographics shown in Table 2). While the initial target enrollment was 25 participants (as outlined in the clinicaltrials.com registration, NCT06234930), the study employed an adaptive design, enabling the assessment of the primary outcomes (modulation of gamma activity, safety and tolerability) at $n = 15$ participants. Inclusion criteria required participants to have a Montreal Cognitive Assessment (MoCA) score equal or above 26, at least 8 years of formal education, fluency in English, and sufficient vision and hearing ability to engage with the study tasks. Participants were excluded if they had: received Memantine treatment in the past 30 days; initiated treatment with acetylcholinesterase inhibitors within the past 30 days; a history of seizure or epilepsy (including a family history of such conditions); a history of stroke; an active diagnosis of migraine headache; diagnosis of mild Alzheimer's disease or related dementias, or a Geriatric Depression Scale (GDS) score greater than 8. Sufficient vision and hearing to participate in our study were determined by a calibration session where participants had to repeat sentences played to them through the VR headset and describe images displayed via the VR screen.

Materials
Participants received multisensory stimulation through a VR headset (Meta Quest 2), tethered to a computer. Visual stimuli were delivered via the VR headset display, while auditory stimuli were presented through headphones (SONY MDR-EX15LP) connected to the headset.

To evaluate the device's performance in delivering synchronized and stable audiovisual stimuli, stability tests were conducted pre- and post-experimental sessions, as it was not physically feasible to record this data during the experimental session. An Arduino Nano microcontroller was used to facilitate the audio and visual recordings of the stimulation. To capture auditory outputs from the VR headset, we interfaced the Arduino board with the headset via a 3.5 mm audio jack. For visual signal measurements, a TEMT6000 photosensor was employed to detect brightness levels from the VR headset's display.

Visual and auditory stimuli were varied depending on the experiment, but the subtended flickered visual field was kept constant across the whole study, comprehending a 54.5° diagonal visual field (48.7° horizontal, 28.6° vertical). Videos and sounds were loaded to the device with their brightness and volume premodulated by

a 40 Hz sine wave. The overall VR headset sound volume level was adjusted to each participant's comfort level. All auditory stimuli were loudness-normalized to -14 Loudness Units Full Scale (LUFS) to ensure consistent perceived volume across conditions, with a 100ms linear fade-in and fade-out to minimize the startle effect.

To assess the neural effects of VR-based gamma sensory stimulation, EEG was selected for its non-invasive nature and capacity to monitor cortical responses in real time. Recordings were collected using the 64 channel BioSemi ActiveTwo system (BioSemi, Amsterdam, the Netherlands). Electrode positions followed the 64 standard equidistant BioSemi sites; however, the five most frontal electrodes (AF7, FP1, FPz, FP2, AF8) were removed to ensure participant comfort, as the top edge of the VR headset overlapped with these positions. Electrooculography (EOG) generated from eye movements and blinks were recorded from two additional electrodes placed approximately 1 cm to the left of the left eye and 1 cm to the right of the right eye. Data was digitized using the BioSemi ActiView software, with a sampling rate of 2048 Hz. Offline analyses were performed with MNE-Python[54].

Experimental tasks

Testing changes in gamma activity in response to 40 Hz stimuli

To evaluate the feasibility of using a VR-based gamma sensory stimulation protocol to drive neural activity at gamma frequencies, we designed three complementary experiments. Experiment 1 focused on assessing the isolated effects of unimodal auditory and visual stimulation delivered by VR on neural activity. Experiment 2 aimed to disentangle gamma stimulus-driven gamma synchronization from endogenous sensory processing by comparing neural responses to 40 Hz-modulated multimedia content against an unmodulated sham condition. Finally, Experiment 3 investigated whether modulation of gamma activity could be achieved with more complex, multimodal audiovisual stimuli delivered during a cognitively engaging associative memory task. Together, these experiments systematically assessed the efficacy and flexibility of VR-based gamma sensory stimulation.

Experiment 1 - passive unimodal 40 Hz VR-based stimulation

This experiment aimed to test the feasibility of delivering unimodal gamma stimulation—either auditory or visual—using VR technology. Participants were exposed to 40 Hz modulated auditory or visual stimuli in isolation, allowing us to evaluate the capacity of each modality to evoke gamma-band neural activity when presented via VR. In addition, we directly compared the effects of simple (e.g., clicks, black-and-white video) and complex (e.g., pure tones, bright videos) stimuli to assess how stimulus complexity influences the magnitude of evoked gamma responses. To do so, a total of 100 trials were conducted, evenly divided between visual and auditory conditions, with each trial lasting 3 s and separated by a jittered inter-trial interval of 3.5 to 4 s. During the inter-trial interval, a black screen with a white fixation cross at the center was displayed to maintain participant focus. Visual stimulation, with brightness sinusoidally modulated between 0% and 100% at 40 Hz (pixel brightness range: 0–255), consisted of 50 trials split into two categories: 25 trials of a plain white rectangle with an average pixel brightness of 255 (referred to as the black-and-white video), and 25 trials of neutral-valence videos, five distinct videos repeated five times each, with an average brightness of 194.41 (referred to as random bright videos). Auditory stimulation also consisted of 50 trials, comprising 25 trials of isochronous 40 Hz click trains characterized by waveforms with 0ms rise/fall times and 1ms plateau durations (similar to prior work by[55]and referred to as clicks); and 25 trials of amplitude-modulated pure tones at 40 Hz, featuring five distinct carrier frequencies evenly spaced between 196 Hz and 1000 Hz, each repeated five times (referred to as pure tones). This experimental design systematically tested the ability of controlled unimodal conditions to drive gamma neural activity, allowing for a comparison of simple and complex sensory stimuli in both visual and auditory modalities.

Experiment 2 - passive multimodal 40 Hz VR-based stimulation

This experiment aimed to confirm that the increases in gamma-band neural activity observed during 40 Hz audiovisual stimulation were driven by the external rhythmic modulation itself, rather than by endogenous processing of the multimedia content. Participants passively viewed and listened to the same video stimulus under four modulation conditions: 40 Hz (active), sham (no modulation), 4 Hz, and a mixed 4–40 Hz pattern. For the present analysis, we focused on the 40 Hz and sham conditions, which directly address the primary hypothesis of gamma evoked activity via VR-based stimulation. The additional conditions (4 Hz and 4-40 Hz) will be explored in future work. The visual content of the movie had an average pixel brightness of 177.5, while the auditory stimuli consisted of a 196 Hz pure tone amplitude-modulated at the relevant frequency. Each stimulation condition included 15 trials, with each trial lasting 5 s separated by a jittered inter-trial interval lasting between 5.5 and 6.5 s. During the inter-trial interval, an immersive black screen was displayed with a white fixation cross at the center. Conditions were randomly displayed to avoid an order effect.

Experiment 3 - active multimodal 40 Hz VR-based stimulation

In Experiment 3, we aimed to determine whether loosely controlled multimedia content—defined here as audiovisual stimuli with naturally varying characteristics, such as brightness, auditory frequency range, and complexity—modulated at 40 Hz and integrated into an associative memory task could induce a significant increase in gamma neural activity compared to the sham condition (no modulation).

To achieve this, we adapted a video-sound associative memory task previously used in sensory stimulation research[29,47,56]. Participants were instructed to focus on and memorize video-sound pairs that were either modulated at 40 Hz and lasted 3 s (stimulation condition) or unmodulated and lasted 1.5 s (sham condition) - a strategy used to balance the amount of information conveyed to the participant across the two conditions. The videos used were of neutral valence and varied significantly in their average brightness (60.78–182.93). To ensure comparability, the distribution of the average pixel brightness of videos used in the 40 Hz stimulation condition

was matched to the average pixel brightness of the videos used in the sham condition (respective means and standard deviation: 105.05 ± 23.45 and 107.4 ± 23.57, t-test=-0.598, $p = 0.551$). Auditory stimuli were drawn from four distinct categories—piano keys, orchestra, acoustic guitar, and electric guitar— with an equal number of sound types used in both the active and sham conditions. The sounds' spectral entropy, a normalized metric where 0 indicates minimal complexity and 1 indicates high complexity, ranged from 0.19 to 0.67, reflecting the diverse sound characteristics used in the task.

Immediately following each video-sound pair association, participants verbally rated how well the video matched the sound on a 5-point scale, where 1 indicated "very poorly" and 5 indicated "very well". Following their response, an inter-trial interval of 1–3 s occurred, during which a white fixation cross was displayed. After every 12 trials in the encoding phase, participants completed a distractor task which involved a visual search task (counting specific target objects among distractors on a table) that lasted 1 min before entering the recall phase. During the recall phase, one of the previously played sounds was played again and three images were displayed simultaneously. The participants were then asked to select out of the three images the one that corresponded to the video previously played with the sound. Of the three options, one was the correct match, one was a foil (an image never shown during the encoding phase), and one was a lure (an image presented earlier but not associated with the current sound).

By assessing neural responses under these more naturalistic and engaging multimodal conditions, this experiment was design to evaluate the robustness of VR-based stimulation for enhancing gamma oscillatory activity during a cognitively loaded task.

Testing safety and tolerability

After completing all experimental tasks and removing the VR headset and EEG cap, participants completed a digital questionnaire to evaluate the safety and tolerability of the VR-based GSS protocol. The questionnaire assessed potential side effects, including headaches, eye pain, disorientation, and nausea, as well as measures of tolerability, such as comfort, enjoyment, and the perceived intensity of the VR experience. Participants rated the severity of side effects on a scale from 0 to 3, where 0 indicated "not at all," 1 indicated "mild," 2 indicated "moderate," and 3 indicated "severe". To measure participants' comfort, enjoyment, and tolerance of various aspects of the protocol and the VR headset, responses were recorded using a 7-point Likert scale. Here, 1 represented the lowest level (e.g., "not at all"), and 7 represented the highest level (e.g., "extremely").

Testing stability of VR-based stimuli delivery system

To evaluate the performance of the off-the-shelf VR devices used in our experiments ($n = 2$, alternated between consecutive participants), we conducted stimulation stability tests and quantified the stability of our 40 Hz visual and auditory stimulation, as well as the synchronization between audiovisual stimuli (as required in Experiments 2 and 3). These tests were performed twice for each participant: once before the recording session began and again after the session ended.

For these tests, an Arduino device was used to collect two types of signals: the voltage fluctuations corresponding to the sound output from the VR headset and the brightness of the VR display using a photodiode. The experiment involved displaying the same movie used in Experiment 2, with its brightness and sound amplitude modulated at 40 Hz with 100% depth. Data were recorded across 25 trials, each lasting 1 s with 3 s between trials.

Results across all participants and trials indicated stable delivery of stimuli. For visual stimuli, the average peak frequency in the power spectral density was 39.95 ± 0.67 Hz, while for auditory stimuli, it was 40.43 ± 0.52 Hz. The delay between audio and visual stimulus onset was -8.8 ± 5.0 ms, with negative values indicating that the visual stimulus preceded the audio stimulus. Phase consistency, measured as PLV between a simulated 40 Hz sinusoidal wave and individual trials, was 0.65 ± 0.16 for visual stimuli and 0.92 ± 0.03 for auditory stimuli. PLV between audio and visual data was on average 0.68 ± 0.16. Importantly, none of these metrics varied significantly between pre- and post-session tests ($p = 0.503$ and $p = 0.486$ for audio and visual PLV, respectively and $p = 0.137$ for PLV between auditory and visual stimuli data).

Although real-time device performance data could not be collected during experimental sessions due to form factor limitations, these stability tests confirm that the VR-based stimuli maintained an average periodicity at the frequency of interest, i.e., 40 Hz, which we expect to have been maintained across the study as these metrics did not vary significantly between pre and post session. Together these findings validate the reliability of our VR-based software system in generating periodic 40 Hz audiovisual stimuli, ensuring the integrity of the experimental protocol.

Metrics to evaluate neural responses to sensory stimuli

EEG preprocessing

All EEG data underwent identical preprocessing steps. The raw signals were initially subjected to a notch filter at 60 Hz and 120 Hz using a finite impulse response (FIR) filter to eliminate power line noise and its harmonics. Subsequently, a band-pass FIR filter was applied with cutoff frequencies set at 1 Hz and 100 Hz to retain the relevant EEG frequency range while removing low-frequency drifts and high-frequency noise. The data were then resampled to a sampling frequency of 1024 Hz to enhance the computational efficiency. To standardize the reference across all recordings, the EEG signals were re-referenced to average reference.

An independent Component Analysis (ICA) was then applied to the data using 30 components, and components were automatically classified using the ICLabel[57]. Components representing muscle artifacts, eye movements, heart activity, channel noise, and line noise were automatically identified and excluded from the data. Across all participants ($N = 16$), an average of 13.8 ± 5.2 independent components were removed. Specifically, muscle artifacts accounted for 8.9 ± 5.5 components, eye movement artifacts for 2.0 ± 0.8 components, and

cardiac artifacts for 0.0 ± 0.0 components per participant. Following ICA cleaning, epoch-level artifact rejection was performed using the AutoReject algorithm[58] which automatically determines optimal rejection thresholds for each channel and participant. AutoReject identified and removed epochs containing residual artifacts while interpolating bad channels within retained epochs. On average, 3.5% of epochs were rejected per participant (median = 1%, range = 0–22%), and an average of 6.1 ± 5.3 channels per epoch were interpolated in the remaining clean epochs.

To quantify stimulus-evoked responses at the sensor level, we used a two-step electrode selection strategy. First, anatomically relevant regions were defined following previous literature[59,60]: frontocentral electrodes for auditory stimulation (overlying auditory cortex and superior temporal areas) and parietooccipital electrodes for visual stimulation (over visual cortex). Second, within each region, we selected the four electrodes showing the strongest gamma-band modulation (30–50 Hz) across all stimulation trials and participants. Modulation was quantified as the change in power spectral density (PSD) at 40 Hz during stimulation relative to a pre-stimulus baseline, using Welch's method. This procedure consistently identified FCz, C2, C1, and Cz for auditory analysis, and Oz, PO3, PO4, and POz for visual analysis. For multimodal and sham conditions, both electrode sets were used.

Power spectral density (PSD)
Power spectral density estimates were obtained using the Welch's method as implemented in the MNE-Python package. The data were segmented into 2048-sample overlapping windows (50% overlap) multiplied by a Hanning tapering function prior to computing the Fourier transform. The resulting periodograms were averaged to yield stable PSD estimates. This approach reduces spectral variance while maintaining adequate frequency resolution, facilitating a more robust characterization of the underlying neural dynamics.

Wavelet power analysis
Gamma power was computed by convolving each EEG signal with a family of Morlet wavelets across (38–42 Hz). Specifically, the Morlet transform decomposes the signal into time-frequency space, and the squared magnitude of the resulting complex coefficients corresponds to the instantaneous power at each time point and frequency. These instantaneous power values are then averaged or integrated within the relevant time windows (e.g., baseline vs. stimulation intervals) to yield a final power estimate for each condition and gamma frequency band of interest. To evaluate stimulus-related changes in power at 40 Hz, we compared power values between a baseline period and the stimulus presentation period. To account for the varying active and inter-trial intervals across the experimental tasks, different baseline windows were defined: -1 to 0 s relative to stimulus onset for Experiment 1, -4.5 to -0.75 s for Experiment 2, and − 2 to 0 s for Experiment 3. Similarly, the stimulus presentation period was defined as 0.75 to 2.5 s for Experiment 1, 0.75 to 4.5 s for Experiment 2, and 0.75 to 2.5 s for Experiment 3. We initiated the stimulus presentation analysis window at 0.75 s post-stimulus onset. This delay was implemented to minimize contamination from early event-related potentials (ERPs), thereby isolating sustained neural responses from transient, stimulus-locked activity. The resulting power values were averaged across the selected channels for each condition.

Inter-trial phase coherence (ITPC)
ITPC was computed using the MNE-Python package which implemented Morlet wavelet transformations. The analytical procedure involved convolving the selected EEG channels (mentioned above) and the specified time interval epochs with complex Morlet wavelets to derive the time-frequency representation, yielding both amplitude and phase information at each temporal and spectral point. An ITPC value was then computed by subsequently averaging the phase components across trials. The ITPC at a given frequency f and time point t was defined as:

$$ITPC\ (f,\ t) = \frac{1}{N}\left|\sum\nolimits_{k=1}^{N} e^{i\theta_k(f,t)}\right|$$

Where f is frequency of interest, t is time point of interest, N is number of trials, $\theta_k(f,t)$ is phase of the signal in the $k-th$ trial at frequency f and time t and $|.|$ denotes magnitude of the resultant vector.

This methodological approach quantifies the degree to which oscillatory neural activity remains phase-locked across trials in response to external stimuli, providing insights into the temporal dynamics of neural synchronization. To evaluate stimulus-related changes in phase coherence, we compared ITPC values between a baseline period (-1 to 0 s relative to stimulus onset for experiment 1, -4.5 to -0.75 s for experiment 2 and − 2 to 0 s for experiment 3) and the stimulus presentation period (0.75 to 2.5 s and 0.75 to 4.5 for experiment 1 and 3 an experiment 2, respectively). The resulting values were averaged across the frequency range of interest (38–42 Hz) and across the selected channels for each condition.

Fold change (FC)
Similar to prior work[27,40] to facilitate the direct interpretation of our results, significant effects of VR-based GSS on neural activity were quantified using the fold change in power and ITPC at the stimulation frequency. The Fold Change was calculated as the ratio of ITPC or power values during the stimulation period to the corresponding values in the baseline period, as shown in the equation below. Subsequently, we subtracted 1 from this ratio yielding a unitless measure centered around zero, where positive values indicate an increase from baseline, and negative values indicate a decrease from baseline.

$$\textbf{Fold Change} = (\textbf{Stimulation Period} / \textbf{Baseline Period}) - 1$$

Time frequency analysis

Time-frequency representations of power and ITPC were computed using the Stockwell transform (S-transform) as implemented in the MNE-Python package. The S-transform was applied across a frequency range of 1–85 Hz, with a width parameter of 0.5 to balance temporal and frequency resolution. For both power and ITPC analyses, the temporal resolution was reduced by a factor of 3 (decim = 3) to enhance computational efficiency. Power spectrograms were calculated as the squared magnitude of the S-transform coefficients and then converted to decibels (dB) using a log-ratio transformation relative to a baseline period of -4.5 to -0.75 s in Experiment 2. ITPC was computed by first normalizing the complex S-transform coefficients to unit magnitude for each trial and then averaging these normalized coefficients across trials. This resulted in a measure of phase consistency ranging from 0 to 1.

Source level analysis

In this study, we applied the Dynamic Imaging of Coherent Sources (DICS) beamformer method (as implemented in MNE-Python) to localize induced gamma-band activity (38–42 Hz) of unimodal stimuli (Experiment 1) to cortical regions. First, we loaded epoched EEG data from − 1 to 3 s relative to stimulus onset and co-registered these data to the fsaverage template brain (Freesurfer) by computing a forward solution, ensuring consistency across participants. We then computed cross-spectral density (CSD) matrices using Morlet wavelets (decimated by a factor of 20), and optimized the DICS filter parameters by conducting an exhaustive search over multiple regularization values combined with five-fold cross-validation. Using the optimal filter, we estimated source power during both the baseline (− 1 to 0 s) and activation (0.75 to 2.5 s) periods for each epoch. We then calculated the log-ratio (in decibels) of the activation power relative to baseline power and morphed these estimates to the fsaverage brain. Finally, individual source estimates were averaged to generate a grand-average source map, which served as the basis for visualizing the spatial distribution of gamma-band activity.

Statistical analysis

In this study, we employed a range of statistical tests to test the significance of change in gamma power and phase alignment from baseline, within and across conditions. We first assessed the normality of each dataset using the Shapiro-Wilk test. For paired comparisons, such as baseline versus stimulation, we used a paired t-test (or one-sample t-test if appropriate) if the data were normally distributed and a Wilcoxon signed-rank test if they were not, to calculate p-values. For comparisons between independent groups, such as two different experimental conditions, we again assessed normality and then used either an independent-samples t-test for normally distributed data or a Mann-Whitney U test for non-normally distributed data. When evaluating a single condition against a theoretical value, like a fold change of 0, we used a one-sample t-test or a Wilcoxon signed-rank test, depending on the data's normality. Significant differences are indicated in the figures with their corresponding p-values, using asterisks to denote the level of significance (* for $p < 0.05$, ** for $p < 0.01$, *** for $p < 0.001$).

Data availability

The data that support the findings of this study are available from the corresponding author (Carolina Reis; carolina@clarity-technologies.com) upon reasonable request.

References

1. Tahami Monfared, A. A., Byrnes, M. J., White, L. A. & Zhang, Q. The humanistic and economic burden of alzheimer's disease. *Neurol. Ther.* **11**, 525–551 (2022).
2. Crews, L. & Masliah, E. Molecular mechanisms of neurodegeneration in alzheimer's disease. *Hum. Mol. Genet.* **19**, R12–R20 (2010).
3. Singh, D. Astrocytic and microglial cells as the modulators of neuroinflammation in alzheimer's disease. *J. Neuroinflammation.* **19**, 1–15 (2022).
4. Tarasoff-Conway, J. M. et al. Clearance systems in the brain-implications for alzheimer disease. *Nat. Rev. Neurol.* **11**, 457–470 (2015).
5. Sims, J. R. et al. Donanemab in early symptomatic alzheimer disease: the TRAILBLAZER-ALZ 2 randomized clinical trial. *JAMA* **330**, 512–527 (2023).
6. van Dyck, C. H. et al. Lecanemab in early alzheimer's disease. *N Engl. J. Med.* **388**, 9–21 (2023).
7. Benussi, A. et al. Increasing brain gamma activity improves episodic memory and restores cholinergic dysfunction in alzheimer's disease. *Ann. Neurol.* **92**, 322–334 (2022).
8. Jones, K. T., Ostrand, A. E., Gazzaley, A. & Zanto, T. P. Enhancing cognitive control in amnestic mild cognitive impairment via at-home non-invasive neuromodulation in a randomized trial. *Sci. Rep.* **13**, 7435 (2023).
9. Jung, Y. H. et al. Effectiveness of personalized hippocampal Network–Targeted stimulation in alzheimer disease: A randomized clinical trial. *JAMA Netw. Open.* **7**, e249220 (2024).
10. Koch, G. et al. Precuneus magnetic stimulation for alzheimer's disease: a randomized, sham-controlled trial. *Brain* **145**, 3776–3786 (2022).
11. Pileckyte, I. & Soto-Faraco, S. Sensory stimulation enhances visual working memory capacity. *Commun. Psychol.* **2**, 1–18 (2024).
12. Chan, D. et al. Gamma frequency sensory stimulation in mild probable alzheimer's dementia patients: results of feasibility and pilot studies. *PloS One.* **17**, e0278412 (2022).
13. Cimenser, A. et al. Sensory-Evoked 40-Hz gamma oscillation improves sleep and daily living activities in alzheimer's disease patients. *Front. Syst. Neurosci.* **15**, 746859 (2021).
14. Da, X. et al. Noninvasive gamma sensory stimulation May reduce white matter and Myelin loss in alzheimer's disease. *J. Alzheimers Dis. JAD.* **97**, 359–372 (2024).
15. Hajós, M. et al. Safety, tolerability, and efficacy estimate of evoked gamma Oscillation in mild to moderate alzheimer's disease. *Front Neurol* **15**, (2024).

16. Fries, P. Rhythms for cognition: communication through coherence. *Neuron* **88**, 220–235 (2015).
17. Jensen, O., Kaiser, J. & Lachaux, J. P. Human gamma-frequency oscillations associated with attention and memory. *Trends Neurosci.* **30**, 317–324 (2007).
18. Gregoriou, G. G., Gotts, S. J., Zhou, H. & Desimone, R. High-frequency, long-range coupling between prefrontal and visual cortex during attention. *Science* **324**, 1207–1210 (2009).
19. Baldauf, D. & Desimone, R. Neural mechanisms of Object-Based attention. *Science* **344**, 424–427 (2014).
20. Kurimoto, R. et al. Induced oscillatory responses during the sternberg's visual memory task in patients with alzheimer's disease and mild cognitive impairment. *NeuroImage* **59**, 4132–4140 (2012).
21. Mably, A. J. & Colgin, L. L. Gamma oscillations in cognitive disorders. *Curr. Opin. Neurobiol.* **52**, 182–187 (2018).
22. Iaccarino, H. F. et al. Gamma frequency entrainment attenuates amyloid load and modifies microglia. *Nature* **540**, 230–235 (2016).
23. Liu, Q. et al. Intensity-dependent gamma electrical stimulation regulates microglial activation, reduces beta-amyloid load, and facilitates memory in a mouse model of alzheimer's disease. *Cell. Biosci.* **13**, 138 (2023).
24. Martorell, A. J. et al. Multi-sensory gamma stimulation ameliorates Alzheimer's-Associated pathology and improves cognition. *Cell* **177**, 256–271e22 (2019).
25. Murdock, M. H. et al. Multisensory gamma stimulation promotes glymphatic clearance of amyloid. *Nature* **627**, 149–156 (2024).
26. Williams, S. D. et al. Neural activity induced by sensory stimulation can drive large-scale cerebrospinal fluid flow during wakefulness in humans. *PLOS Biol* **21**, (2023).
27. Blanpain, L. T. et al. Multisensory flicker modulates widespread brain networks and reduces interictal epileptiform discharges. *Nat. Commun.* **15**, 3156 (2024).
28. Headley, D. B. & Weinberger, N. M. Gamma-Band activation predicts both associative memory and cortical plasticity. *J. Neurosci.* **31**, 12748–12758 (2011).
29. Wang, D., Shapiro, K. L. & Hanslmayr, S. Altering stimulus timing via fast rhythmic sensory stimulation induces STDP-like recall performance in human episodic memory. *Curr. Biol.* **33**, 3279–3288e7 (2023).
30. Hanslmayr, S., Axmacher, N. & Inman, C. S. Modulating human memory via entrainment of brain oscillations. *Trends Neurosci.* **42**, 485–499 (2019).
31. Hajós, M. et al. Safety, Tolerability and efficacy of 40Hz sensory stimulation for Alzheimer's disease. 03.23.23287637 Preprint at (2023). https://doi.org/10.1101/2023.03.23.23287637 (2023).
32. de Vries, E. & Baldauf, D. Attentional weighting in the face processing network: A magnetic response Image-guided magnetoencephalography study using multiple Cyclic entrainments. *J. Cogn. Neurosci.* **31**, 1573–1588 (2019).
33. Tabarelli, D., Keitel, C., Gross, J. & Baldauf, D. Spatial attention enhances cortical tracking of quasi-rhythmic visual stimuli. *NeuroImage* **208**, 116444 (2020).
34. Khachatryan, E. et al. Cognitive tasks propagate the neural entrainment in response to a visual 40 hz stimulation in humans. *Front. Aging Neurosci.* **14**, 1010765 (2022).
35. Lahijanian, M., Aghajan, H. & Vahabi, Z. Auditory gamma-band entrainment enhances default mode network connectivity in dementia patients. *Sci. Rep.* **14**, 13153 (2024).
36. Jones, M. et al. Gamma band light stimulation in human case studies: groundwork for potential alzheimer's disease treatment. *J. Alzheimers Dis. JAD.* **70**, 171–185 (2019).
37. Bohil, C. J., Alicea, B. & Biocca, F. A. Virtual reality in neuroscience research and therapy. *Nat. Rev. Neurosci.* **12**, 752–762 (2011).
38. Riva, G., Wiederhold, B. K. & Mantovani, F. Neuroscience of virtual reality: from virtual exposure to embodied medicine. *Cyberpsychology Behav. Soc. Netw.* **22**, 82–96 (2019).
39. Bartoli, E. et al. Functionally distinct gamma range activity revealed by stimulus tuning in human visual cortex. *Curr. Biol. CB.* **29**, 3345–3358e7 (2019).
40. Duecker, K., Gutteling, T. P., Herrmann, C. S. & Jensen, O. No evidence for entrainment: endogenous gamma oscillations and rhythmic flicker responses coexist in visual cortex. *J. Neurosci.* **41**, 6684–6698 (2021).
41. Lachaux, J. P. et al. The many faces of the gamma band response to complex visual stimuli. *NeuroImage* **25**, 491–501 (2005).
42. Tallon-Baudry, C., Bertrand, O., Peronnet, F. & Pernier, J. Induced γ-Band activity during the delay of a visual Short-Term memory task in humans. *J. Neurosci.* **18**, 4244–4254 (1998).
43. He, Q. et al. A feasibility trial of gamma sensory flicker for patients with prodromal alzheimer's disease. *Alzheimers Dement. Transl. Res. Clin. Interv.* **7**, e12178 (2021).
44. Liu, C. et al. Modulating gamma oscillations promotes brain connectivity to improve cognitive impairment. *Cereb. Cortex N Y N 1991.* **32**, 2644–2656 (2022).
45. Nissim, N. R., Pham, D. V. H., Poddar, T., Blutt, E. & Hamilton, R. H. The impact of gamma transcranial alternating current stimulation (tACS) on cognitive and memory processes in patients with mild cognitive impairment or alzheimer's disease: A literature review. *Brain Stimulat.* **16**, 748–755 (2023).
46. Nyhus, E. & Curran, T. Functional role of gamma and theta oscillations in episodic memory. *Neurosci. Biobehav Rev.* **34**, 1023–1035 (2010).
47. Wang, D., Clouter, A., Chen, Q., Shapiro, K. L. & Hanslmayr, S. Single-Trial phase entrainment of theta oscillations in sensory regions predicts human associative memory performance. *J. Neurosci.* **38**, 6299–6309 (2018).
48. Hoyer, R. S. et al. Valence-dependent sensory-rhythmic neural entrainment modulates cortico-subcortical dynamics, attention, and memory. 01.03.631218 Preprint at (2025). https://doi.org/10.1101/2025.01.03.631218 (2025).
49. Arlati, S. et al. Acceptance and usability of immersive virtual reality in older adults with objective and subjective cognitive decline. *J. Alzheimers Dis. JAD.* **80**, 1025–1038 (2021).
50. Bauer, A. C. M. & Andringa, G. The potential of immersive virtual reality for cognitive training in elderly. *Gerontology* **66**, 614–623 (2020).
51. Wais, P. E., Arioli, M., Anguera-Singla, R. & Gazzaley, A. Virtual reality video game improves high-fidelity memory in older adults. *Sci. Rep.* **11**, 2552 (2021).
52. Ziegler, D. A. et al. Leveraging technology to personalize cognitive enhancement methods in aging. *Nat. Aging.* **2**, 475–483 (2022).
53. Chattha, U. A. et al. Motion sickness in virtual reality: an empirical evaluation. *IEEE Access.* **8**, 130486–130499 (2020).
54. Gramfort, A. et al. MEG and EEG data analysis with MNE-Python. *Front Neurosci.* **7**, (2013).
55. Arnal, L. H., Kleinschmidt, A., Spinelli, L., Giraud, A. L. & Mégevand, P. The rough sound of salience enhances aversion through neural synchronisation. *Nat. Commun.* **10**, 3671 (2019).
56. Clouter, A., Shapiro, K. L. & Hanslmayr, S. Theta phase synchronization is the glue that binds human associative memory. *Curr. Biol.* **27**, 3143–3148e6 (2017).
57. Pion-Tonachini, L., Kreutz-Delgado, K. & Makeig, S. ICLabel: an automated electroencephalographic independent component classifier, dataset, and website. *NeuroImage* **198**, 181–197 (2019).
58. Jas, M. et al. Automated artifact rejection for MEG and EEG data. *NeuroImage* **159**, 417–429 (2017).
59. McFadden, K. L. et al. Test-Retest reliability of the 40 hz EEG auditory Steady-State response. *PLOS ONE.* **9**, e85748 (2014).
60. Herrmann, C. S. Human EEG responses to 1–100 hz flicker: resonance phenomena in visual cortex and their potential correlation to cognitive phenomena. *Exp. Brain Res.* **137**, 346–353 (2001).

Author contributions

Conceptualization: C.R., T.Z., and A.C.; Methodology: C.R., A.C., and S.H.; Software: G.H. and C.R.; Formal Analysis: H.A. and C.R.; Investigation: G.H., S.N., and C.R.; Resources: R.C.; Data Curation: G.H. and H.A.; Writing – Original Draft: C.R. and H.A.; Writing – Review and Editing: H.A., G.H., S.N., R.C., T.Z., A.C., and S.H.; Supervision: C.R.

Declarations

Competing interests

H.A., G.H., S.N., and C.R. are employees of Clarity Health Technologies and hold stock options in the company. R.C. is the founder and CEO of Clarity Health Technologies, Inc. and holds stock in the company. S.H., A.C., and T.Z. serve as scientific advisers to Clarity Health Technologies, Inc. and hold stock in the company.

Additional information

Correspondence and requests for materials should be addressed to C.R.

Reprints and permissions information is available at www.nature.com/reprints.

Publisher's note Springer Nature remains neutral with regard to jurisdictional claims in published maps and institutional affiliations.